Ni,Zn/SiO₂ FERRITE NANOCOMPOSITES PREPARED BY AN IMPROVED SOL-GEL METHOD AND THEIR CHARACTERISATION

M. Stefanescu[*], C. Caizer[a], M. Stoia, O. Stefanescu

„Politehnica" University of Timisoara, Faculty of Chemistry and Chemical Engineering, P. Victoriei no. 2, 1900-Timisoara, Romania
[a]West University of Timisoara, Faculty of Physics, Department of Electricity and Magnetism, Bd. Parvan no. 4, 1900-Timisoara, Romania

Ni,Zn/SiO₂ nanocomposites with magnetic properties were obtained by an improved sol-gel method (hibrid gels) by using $Si(OC_2H_5)_4$ Zn, Ni, Fe, nitrates, ethanol (C_2H_5OH) and ethylene glycol. After drying and calcinations of the gels at temperatures between 600-1300 °C, the reaction products were characterized by thermal analysis, IR-Spectroscopy, X-Ray diffraction and magnetic measurements. Unlike the case when we used only the thermal decomposition of the complex combination with glyoxilate dianion ligand method, in order to obtain nanocrystalline Ni-Zn ferrite, in this case we used a combined method, between the first one and the known sol-gel method. The special result of this proposed method is the producing of ultra fine magnetic nanoparticles, with diameters even smaller than 3.5 nm. The presence of the ferimagnetic phase was clearly evidenced from magnetic measurements starting even from low temperatures (550 °C) for a weight percentage ferrite: SiO₂ of 35:65. The magnetic behaviour of $Zn_xNi_{(1-x)}Fe_2O_4$ (x = 0.35) ferrite nanoparticles, in silica matrix, obtained after thermal treatment at 600 °C in a quasistatic magnetic field (50 Hz), is super paramagnetic for a 3.5 nm mean diameter, respectively ferromagnetic for 6 nm mean diameter.

1. Introduction

Ferrites represent an important category of materials, which are largely used, due to their numerous practical applications, as for example magnetic devices in electronic, optical and microwave installations [1,2]. Most of the physical properties of these materials, especially the magnetic ones (coercivity, saturation magnetization, losses) dramatically change with the decrease of the particle size, until the nano-size [3,4]. Thus, a special interest was paid to the synthesis methods that allow for getting the nanocomposites. In this context, the unconventional synthesis methods [5-8] gained an advantage over the conventional methods [9,10].

One of the most popular unconventional synthesis methods, very much used in the past years is the sol-gel method [11-13]. This method was successfully used in obtaining nanomaterials, especially magnetic nanomaterials – simple ones or included in inorganic matrix. The nanocomposites obtained by including magnetic ferrite nanoparticles in a nonmagnetic matrix using the sol-gel method are of interest due to the new physical, chemical, electrical and magnetic properties resulted from their particulate structure, by comparison with the bulk material [14-16].

In our previous studies we obtained the Ni-Zn ferrite, by an original, unconventional patented method [17] based on the oxidation reaction of ethylene glycol to the glyoxylate dyanion, by the NO_3^- ion, with the formation of the heteropolynuclear complex combination

---

[*] Corresponding author: stefanescu@chem.utt.ro

[$Fe_2Ni_{1-x}Zn_x(OH)_4(C_2H_2O_4)_2 \cdot H_2O$], x=(0÷1) [18-20]. After the thermal decomposition of the mentioned complex combination, the Ni-Zn ferrite is obtained as a very fine powder, even starting at ~400 °C, much lower temperature than by the classical method of annealing mechanical mixtures, where the synthesis temperatures are 1200 °C-1400 °C.

In the present paper we pursued the preparation of the Ni-Zn ferrite as nanoparticles dispersed in a SiO_2 matrix, by combining the original getting method for $Ni_{1-x}Zn_xFe_2O_4$ (x = 0.35) ferrite (by the thermal decomposition of the heteropolynuclear complex combination at low temperatures (550 °C)) with the sol-gel method. This new hybrid synthesis way allowed for getting Ni-Zn ferrite at rather low temperatures and with highly reduced particle diameter (~ 3 nm), dispersed in the silica matrix. The magnetic properties of the samples strongly depend on the dispersion in silica matrix of ferrimagnetic nano particles size.

2. Experimental

2.1. Synthesis

The materials used for the synthesis were: $Fe(NO_3)_3 \cdot 9H_2O$ (Merck), $Ni(NO_3)_2 \cdot 6H_2O$ (Merck), $Zn(NO_3)_2 \cdot 6H_2O$ (Merck), ethylene glycol (p.a.) and tetraethylorthosilicate (TEOS) (Fluka, 98%).

Synthesis I: the synthesis of $Ni_{0.65}Zn_{0.35}Fe_2O_4/SiO_2$ (35% ferrite, 65% SiO_2, mass percents) starting from <u>metallic nitrates, ethylene glycol (EG) and tetraethylorthosilicate (TEOS)</u>.

The metallic nitrates, weighed to the designed stoichiometric ratio, have been dissolved in ethylene glycol (EG) (to obtain a NO_3^-: EG ratio of 1:1) and ethanol. The obtained solution has been slowly added in drops, while stirring, to the ethanol TEOS solution. Ethanol has been added in order to increase the miscibility of the two solutions.

Synthesis II: the synthesis of $Ni_{0.65}Zn_{0.35}Fe_2O_4/SiO_2$ (35% ferrite, 65% SiO_2, mass percents) starting from <u>metallic nitrates, and tetraethylorthosilicate (TEOS)</u>.

The metallic nitrates have been dissolved in ethanol and than added in the same conditions as the previous synthesis, to the ethanol TEOS solution.

Synthesis III: the synthesis of the SiO_2 matrix starting from EG and TEOS.

The ethanol-EG solution has been added under stirring to the ethanol TEOS solution.

The homogenous, clear solutions obtained in all the three syntheses have been left at room temperature and air atmosphere to gellify. The obtained gels have been dried in the drying oven at 60 °C, for 10 hours. After drying and milling, the resulted powders have been thermally treated at different temperatures and than characterized.

Standard complex combination [$Fe_2Ni_{0.65}Zn_{0.35}(OH)_4(C_2H_2O_4)_2 \cdot xH_2O$] was prepared from the corresponding metal nitrates and ethylene glycol, according to our original method described in the previous papers [18-20].

2.2. Experimental techniques

The dried gels and the thermally treated powders from the synthesis have been characterized by thermal analysis and IR spectrometry. The thermal analysis (differential thermal analysis (DTA) and thermogravimetric analysis (TG)) was carried out in unisothermal regime, on Pt plates, in air, using a MOM Budapest 1500-D Derivatograph.

The FT-IR spectra of the powdered samples were carried out with a JASCO 430 FT-IR spectrometer on KBr pellets.

The crystalline phases obtained on the composites were identified by X-ray diffraction in a Bruker and Dron 3 diffractometers using Cu-K_α ($\lambda_{CuK\alpha}$ = 1.54056 Å) and also

Mo-K$_\alpha$ (λ_{Mok} = 0.70930 Å) radiation. The use of Mo-K$_\alpha$ radiation was necessary in order to put in evidence more clearly the material with very small size nanocrystallites.

The magnetic behaviour of the Ni-Zn ferrite nanoparticles, dispersed in the silica matrix was studied at room temperatures and magnetic field frequency of 50 Hz. Magnetic measurements were performed with a standard equipment described in ref. [21] provided with a data acquisition system (DAQ) connected to a personal computer (PC).

3. Experimental results

Obtaining the Ni$_{0.65}$Zn$_{0.35}$Fe$_2$O$_4$ ferrite in SiO$_2$ matrix by the proposed method assumes the formation of the heteropolynuclear complex combination [Fe$_2$Ni$_{0.65}$Zn$_{0.35}$(C$_2$H$_2$O$_4$)$_2$(OH)$_4$·H$_2$O] as an intermediate phase, included in the inorganic matrix, as a result of the redox reaction (equation 1):

$$2Fe(NO_3)_3 + 0.65Ni(NO_3)_2 + 0.35\ Zn(NO_3)_2 + 2\ C_2H_4(OH)_2 + xH_2O\ \rightarrow \qquad (1)$$

$$Fe_2Ni_{0.65}Zn_{0.35}(OH)_4(C_2H_2O_4)_2.xH_2O + 4\ NO + 4\ HNO_3$$
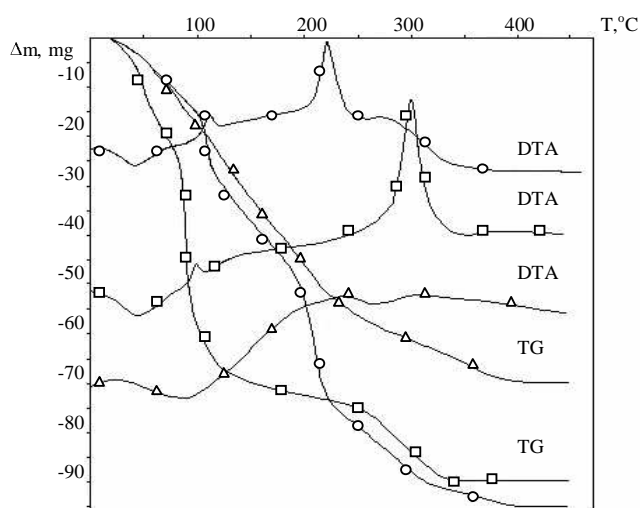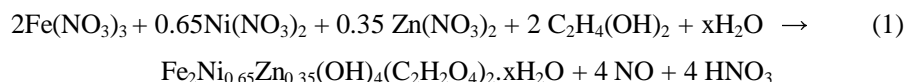
Fig. 1. TG and DTA curve of samples: dried gel at 60 ^{o}C from synthesis I ($\circ$); dried gel at 60 ^{o}C from synthesis II ($\triangle$); a solution metal nitrates–ethylene glycol (NO$_3^-$: EG = 1 : 1) ($\square$).

The formed complex combination leads to the corresponding oxide mixture after the thermal decomposition at ~400 ℃.

In Fig. 1 there are shown the TG and DTA curves of the gels resulted from the synthesis I ($\circ$ curve) respectively synthesis II ($\triangle$ curve), as well as of a metallic nitrates – ethylene glycol solution (in molar ratio NO$_3^-$: EG = 1 : 1) ($\square$ curve).

The formations in the matrix of the heteropolynuclear complex combination, its thermal decomposition and the behaviour during the thermal treatment of the silica matrix system, have been studied by IR spectrometry. The FT-IR spectra are shown in Fig. 2. The frequencies of the IR main absorption bands corresponding to the studied samples and the assignment of these bands are shown in Table 1.

Table 1. IR frequencies of main absorption bands of the studied samples.

| IR frequencies [cm^{-1}]							Assignment
1	2	3	4	5	6	7	
3360	3426	3426	3438	3368	3427	3400	3440 cm^{-1}: $\nu(H_2O)$
2959	2947	2936	-	-	2940	2947	2950 cm^{-1}: $\nu_{as}(CH_2)$
2880	2880	-	-	-	-	2860	2880 cm^{-1}: $\nu(CH)$
1623	1610	1615	1627	1638	1620	-	1640 cm^{-1}: $\delta(H_2O)$
-	-	-	-	-	-	1615	1620 cm^{-1}: $\nu_{as}(COO)$
-	-	1393	-	-	-	1386	1390 cm^{-1}: $\nu_s(COO)$
1380	1380	-	-	1380	-	-	1380 cm^{-1}: (NO_3^-)
-	-	1364	1358	-	-	1358	1360 cm^{-1}: $\delta(OH)$
-	-	1312	1312	-	-	1312	1320 cm^{-1}: $\nu_s(CO)$
-	-	-	-	-	-	1218	1220cm^{-1}:$\nu(OH)+\delta(OH)$
1180	1188	1183	1200	1194	1194	-	1200 cm^{-1}: $\nu_{as}(Si-O-Si)$
-	-	-	-	-	-	1073	1080 cm^{-1}: $\nu(COH)$
1072	1062	1065	1065	1065	1065	-	1075 cm^{-1}: $\nu_{as}(Si-O-Si)$
960	960	-	-	948	950	-	960 cm^{-1}: $\nu(Si-OH)$
792	794	800	800	796	790	-	800 cm^{-1}: $\nu_s(Si-O-Si)$
-	-	-	-	-	-	800	780cm^{-1}: $\delta(OCO)+\nu(MO)$
-	-	-	-	-	-	715	715 cm^{-1}: $\rho(H_2O)$
452	445	446	450	446	434	490	480 cm^{-1}: $\nu(MO)$
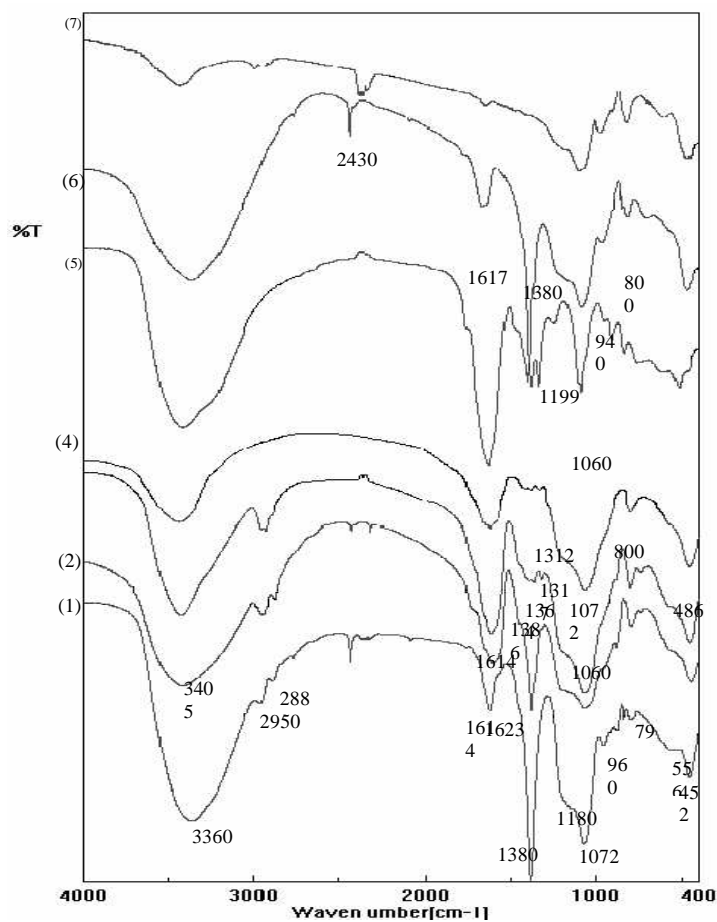
Fig. 2. FT-IR spectra: (1) gel from synthesis I, dried at 25 ^{o}C; (2) gel from synthesis I, dried at 60 ^{o}C; (3) gel from synthesis I, thermally treated at 130 ^{o}C; (4) gel from synthesis I, thermally treated at 200 ^{o}C; (5) standard complex [Fe$_2$Ni$_{0.65}$Zn$_{0.35}$(OH)$_4$(C$_2$H$_2$O$_4$)$_2$.xH$_2$O; (6) gel from synthesis II, thermally treated at 130 ^{o}C; (7) gel from synthesis III, thermally treated at 130 ^{o}C.

Fig. 3 represents the XRD patterns of the samples obtained by synthesis I (spectra (a) and (c)) respectively by synthesis II (spectra (b) and (d)), both after thermal treatment at 800 ^{o}C. Also, the XRD patterns of the sample obtained by synthesis I calcined at 600 ^{o}C are shown in Fig. 3 (spectra e). In order to obtain a better identification of the phase, it was used both Cu-K$_\alpha$ radiation (a and b spectra) and Mo-K$_\alpha$ radiation ((c) and (d) spectra). The XRD patterns of the samples prepared by synthesis I and synthesis II, and fired at 1300 ^{o}C, were recorded. Fig. 4 represents the spectrum of the sample obtained by first synthesis after firing at 1300 ^{o}C. The spectrum of the sample obtained by the second synthesis is almost like the spectrum of sample I with the remark that XRD patterns are narrower and sharper in the case of sample II. The spectra of samples obtained by both syntheses (I and II) recorded with Cu-K$_\alpha$ radiation at 600 ^{o}C show that all phases are quasi-amorphous at this temperature.

The magnetical behaviour of the samples was studied at 600 ^{o}C (Fig. 5). Clear differences were evidenced between samples prepared by synthesis I, and samples prepared by synthesis II, respectively. For both samples (synthesis I and II) at temperature upon 700 ^{o}C, magnetization follows a hysteresis cycle, and increases with temperature.
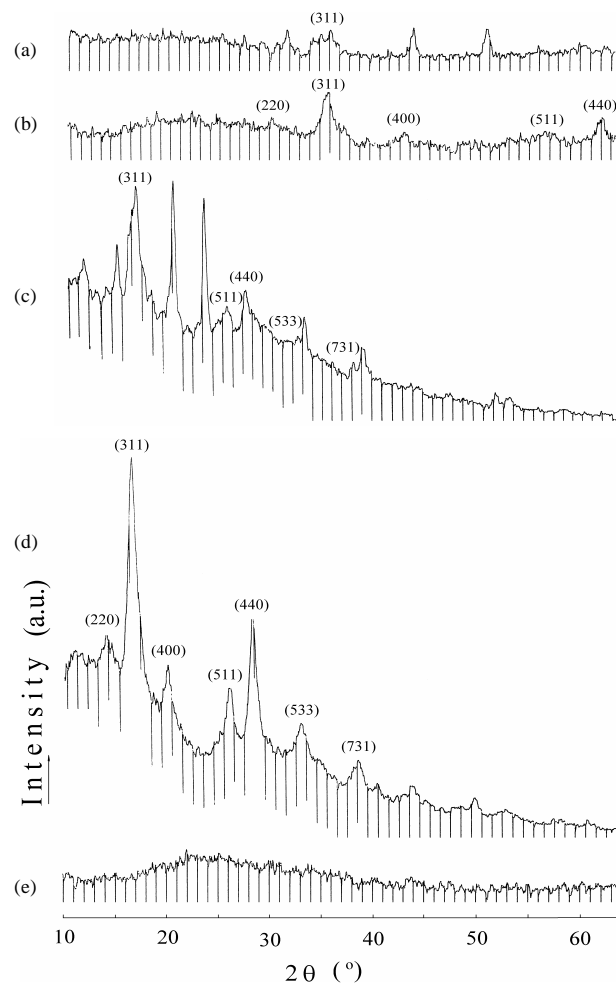

Fig. 3. XRD patterns of samples obtained by synthesis I and II fired at 800 ^{o}C recorded with Cu-K$_\alpha$ radiation ((a) and (b) spectra) and respectively with Mo-K$_\alpha$ radiation ((c) and (d) spectra). XRD spectra of the sample I recorded (with Cu-K$_\alpha$ radiation) after a thermal treatment at 600 ^{o}C (e).
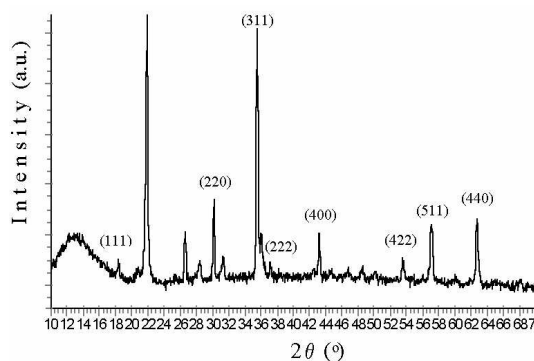
Fig. 4. XRD patterns of sample I, calcined at 1300 °C, recorded with Cu-K$_\alpha$ radiation.
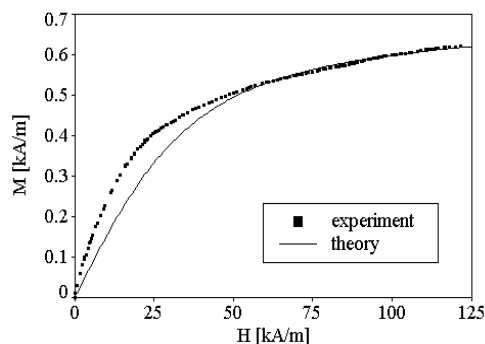

Fig. 6. Theoretical and experimental M – H curve for the sample from synthesis I, fired at 600 °C .
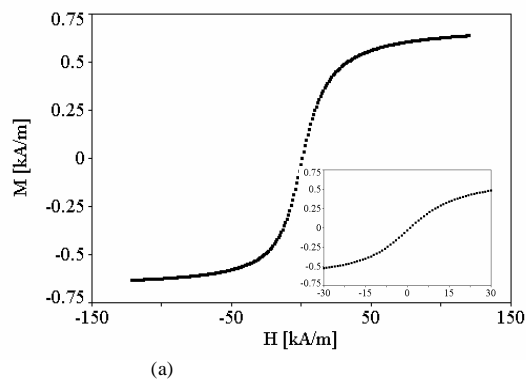

Fig. 5. Magnetization vs. magnetic field for the sample prepared by synthesis I (a) and II (b) fired at 600 °C.

4. Discussions

As we have previously shown [20], from the evolution of the DTA curve (□), Fig. 1, corresponding to the metallic nitrates solution in EG, it may be noticed an exothermal effect at ~100 °C assigned to the redox reaction, when the heteropolynuclear complex combination forms, followed by another exothermal effect at ~ 290 °C, corresponding to the decomposition of the complex combination. Comparing the DTA curve (○) (Fig. 1) corresponding to the gel resulted from the synthesis I (metallic nitrates – EG – TEOS) with the DTA curve (□), there were noticed two similar exothermal effects at ~100 °C, respectively at 230 °C, which can be assigned to the complex combination [Fe$_2$Ni$_{0.65}$Zn$_{0.35}$(C$_2$H$_2$O$_4$)$_2$(OH)$_4$·H$_2$O] (110 °C) formation in the inorganic matrix and its decomposition (230 °C). The complex combination decomposition at lower temperature (230 °C) in the silica matrix is due to the advanced dispersion of the complexes particles inside the matrix. The absence of some similar effects on the DTA curve (Δ) in Fig. 1, corresponding to the gel resulted from synthesis II (metallic nitrates – TEOS) make us to assign them to the formation, respectively the decomposition of the heteropolynuclear complex combination with glyoxilate dyanion is correct.

From the TG curves (○) and (Δ), shown in Fig. 1, it may be noticed that slow mass losses take place slowly, the losses being assigned to the elimination of the (-OH, -OR) residual groups from the silica matrix [22]. The FT-IR spectra (Fig. 2, spectra (1) and (2)) of gels dried at 25 °C and 60 °C respectively, show the characteristic bands assigned to stretching vibrations of silica matrix (Table 1) [23-25] and the strong band from 1380 cm^{-1} assigned to the asymmetric NO$_3^-$ stretching vibration [26]. Upon increasing temperature a drop in band intensity is observed, and, finally, in the spectrum (3) of gel treated at 130 °C this band disappears. The disappearance of the band from 1380 cm^{-1} is due to the NO$_3^-$ ions consumption during the oxidation of ethylene glycol. The presence of the strong band ν_s(NO$_3$) at 1380 cm^{-1} in spectra (6) of the gel treated at 130 °C (obtained from synthesis II – without EG) confirms the disappearance of the complex combination according to equation (1).

Heteropolynuclear complex combination was obtained from the gel dried at 130 ^{o}C. The formation of this complex combination was confirmed by three IR absorption bands which appear in the 1300 – 1400 cm^{-1} region and also by the band from 1615 cm^{-1}. These bands are assigned to v_s (COO), v_s(CO), δ(OH) and v_s(COO) vibrations which are characteristic to carboxylic group of glyoxilate anion. These characteristic bands – presented also in the spectrum (4) of gel (synthesis 1) claimed at 200 ^{o}C – have low intensities as a result of thermal decomposition of complex compound included in silica matrix. In the proposed synthesis conditions (synthesis I: NO$_3^-$, EG, TEOS) and according to literature [27] there is the possibility as ethylene glycol to take part in the condensation reaction by silanol groups, and finally to enter in the silica matrix structure. This assumption is confirmed by the presence in the IR spectra (7) of sample prepared by synthesis III of IR bands in 2800 – 3000 cm^{-1} region assigned to characteristic stretching vibrations of C-H band from CH$_2$ groups [28]. All these adsorption bands are recovered in spectra (1)-(3) of samples prepared by synthesis I.

By indexing the XRD patterns it could be observed the Ni-Zn ferrite formation for the samples resulted through firing at 800 ^{o}C of the gels from synthesis I and II (Fig. 3). The diffraction maximum (311) of sample from synthesis I (Fig. 3 (c)) has a lower intensity, but a full-width at half-maximum larger than the same diffraction maximum of sample from synthesis II (Fig. 3 (d)). All the diffraction peaks have low intensity with the exception of those calcined at 1300 ^{o}C (Fig. 4). In the same time, in the spectrum of the sample from synthesis I, calcined at 800 ^{o}C, there are some unidentified diffraction lines (these lines cannot be attributed to any compounds according to ASTM files) which are absent at low temperatures (600 ^{o}C). These lines could not be found in the spectra of sample from synthesis I calcined at 1300 ^{o}C. The characteristic diffraction lines of β-SiO$_2$ phase were evidenced (Fig. 4). The XRD spectrum of the sample from synthesis II presents the same diffraction lines, but in this case they have higher intensities and lower values of full width at half-maximum. Taking into account that for both samples β-SiO$_2$ phase crystallised at 1300 ^{o}C we suppose that owing to the presence of ethylene glycol even from the starting of silica matrix formation process it could be possible to form a Si-O compound, even at low temperature (800 ^{o}C).

The amorphous features (low and large diffraction maxima) of the sample fired at 800 ^{o}C (Fig. 3. (a) and (b)) show that Ni$_{0.65}$Zn$_{0.35}$Fe$_2$O$_4$ ferrite is presented in the samples as nanoparticles. In order to obtain a better determination of full width at half maximum of diffraction lines, the XRD patterns were recorded by using Mo-K$_\alpha$ radiation (Fig. 3 (c) and (d)).

By using Scherrer formula [29] it was determined that the nanoparticles mean diameter is D$_{I(311)} \cong$ 3.5 nm for sample from synthesis I and D$_{II(311)} \cong$ 6 nm for sample from synthesis II, respectively. So, by using the synthesis II an increase of nanoparticles diameter with 71% was observed. These results prove some real advantages of our method, especially the possibility to obtain finer nanoparticles than those obtained by well-known sol-gel method [30].

The magnetic behaviour of nanocomposites is influenced by the mean diameter size. Thus, owing to higher values of nanoparticles diameter of sample from synthesis II compared with the sample from synthesis I, in the former case the hysteresis loops are presented, while for the other one hysteresis loops are not observed. However, for Ni-Zn ferrite with 3.5 – 6 nm diameter range, the observed behaviour is unusual, as ferrite would exhibit super paramagnetic properties.

According to literature, when nanoparticles are included in silica matrix their magnetic anisotropy exhibits a pronounced increasing (with one, even two orders of magnitude) [31,32]. Thus the energy barrier of magnetic moment becomes comparable or even higher than thermal barriers. Due to above-mentioned effects for magnetic moments it is difficult to overcome the potential barrier (Fig. 6.) or in some cases they could be blocked (especially for nanoparticles with higher diameters) (Fig. 5. (b)). Indeed, even for sample from synthesis I which gives rise to nanoparticles with mean diameter of only 3.5 nm, one gets a deviation of experimental curve (Fig. 6, (■)) from the Langevin theoretical one (Fig. 6. (—)). Also, the magnetization in the field of 130 kA/m is twice higher for nanoparticles of 6 nm (sample from synthesis II) than the magnetization for nanoparticles of 3.5 nm (sample from synthesis I).

5. Conclusions

The proposed method, which is a combination between the thermal decomposition of complex with glyoxilate ligand method and the sol-gel one, allows to obtain ultra fine Ni-Zn ferrite nanoparticles (diameter size under 3.5 nm) inserted on silica matrix at reaction temperature until 550 ^{o}C. This is a real advantage if compared to classical sol-gel method. In the later case, the diameter values of nanoparticles exceeded 6 nm, depending upon working conditions. Moreover,

even in the absence of ethylene glycol (synthesis II) owing to our working condition we have got nanoparticles with average diameter of 6 nm - which is lower than that obtained by others autors (19 nm [13]) at the same ferrite-SiO_2 concentration and same temperature. The magnetic behaviour of nanoparticles is influenced by the mean diameter size. Thus, while the Ni-Zn ferrite nanoparticles of 3.5 nm behave in external magnetic field (ν = 50 Hz) without hysteresis loop and tend to saturation (very close to a soft superparamagnetic material), the nanoparticles with 6 nm diameter presents hysteresis loop without saturation, in the used field of 130 kA/m. This deviation could be attributed to the higher anisotropy of nanoparticles inserted into silica matrix.

Acknowledgements

References

[1] M. Sedlář, V. Matějec, T. Grygar, J. Kadlecová, Ceramics International **26**, 507 (2000).
[2] A. M. Abdeen, J. Magn. Magn. Mater. **185**, 199 (1998).
[3] D. Sen, P. Deb, S. Mazumder, A. Basumallick, Pergamon. Mat. Res. Bull. **35**, 1243 (2000).
[4] J. Shi, S. Gider, K. Babcock, D. D. Awschalorn, Science **271**, 937 (1996)
[5] P. S. Anil Kumar, J. J. Shrotri, S. D. Kulkarni, C. E. Deshapande, S. K. Date, Mat. Lett. **27**, 293 (1996).
[6] A. Verma, T. C. Goel, R. G. Mendiratta, P. Kishan, J. Magn. Magn. Mater. 208, 13 (2001).
[7] J. H. Lee, D. Y. Maeng, Y. S. Kim, C. W. Won, J. Mater. Sci. Lett. **18**, 1029 (1999).
[8] J. S. Jiang, L. Gao, X. L. Yang, J. Mat. Sci. Lett. **18**, 1781 (1999).
[9] D. Segal, J. Mater. Chem. **7(8),** 1297 (1997).
[10] R. G. Gupta, R. G. Mendiratta, J. Appl. Phys. **48**, 845,(1977).
[11] D. H. Chen, X. R. He, Mater. Res. Bull. **36**, 1369 (2001).
[12] M. Politi, C. D. Tran, Journal of Non-Crystalline Solids **304**, 64 (2002)
[13] A. S. Albuquerque, J. D. Ardisson, W. A. A. Macedo, J. Magn. Magn. Mater. **192**, 277 (1999).
[14] X. He, Q. Zhang, Z. Ling, Mater. Lett. **57**, 3031 (2003).
[15] K. Haned, A. H. Morris, J. Appl. Phys. **63**, 4258 (1988).
[16] E. Pammaparayil, R. Marande, S. Komarneni, J. Appl. Phys. **69**, 5349 (1991).
[17] M. Bîrzescu, M. Cristea, M. Ştefanescu, Ghe. Constantin, Rom. Pat. 102501, Sept. 27, (1990).
[18] C. Caizer, M. Ştefanescu, J. Phys. D: Appl. Phys. **35**, 3035 (2002).
[19] C. Caizer, M. Ştefanescu, C. Muntean, I. Hrianca, J. Optoelectron. Adv. Mater. **3(4),** 919 (2001).
[20] M. Ştefanescu, C. Caizer, C. Muntean, M. Stoia, M. Bîrzescu, Chem. Bull. "Politehnica" Univ. (Timisoara) **45(59)**,1, 30 (2000).
[21] C. Caizer, J. Phys.: Condens. Matter **15**, 765 (2003).
[22] M. Zaharescu, M. Crişan, A. Jitianu, D. Crişan, Chem. Bull. "Politehnica" Univ. (Timisoara) **44(58)1**, 53 (1999).
[23] D. C. L. Vasconcelos, W. R. Campos, V. Vasconcelos, W. L. Vasconcelos, Materials Science and Engineering **A 334**, 53 (2002).
[24] C. Savii, M. Popovici, C. Enache, J. Subrt, D. Niznansky, S. Bakardzieva, C. Caizer, I. Hrianca, Solid State Ionics **151**, 219 (2002).
[25] S. Bruni, F. Cariati, M. Casu, A. Lai, A. Musinu, G. Piccaluga, S. Solinas, Nanostruct. Mater. **11(5)**, 573 (1999).
[26] Z. X. Yue, J. Zhou, L. T. Li, H. G. Zhang, Z. L. Gui, J. Magn. Magn. Mater. **208**, 56 (2000).
[27] C. P. Higginbotham, R. F. Browner, J. D. Jenkins, J. K. Rice, Materials Letters **57**, 397 (2003).
[28] R. F. S. Lenza, W. L. Vasconcelos, Journal of Non-Crystalline Solids **330**, 216 (2003).
[29] H. P. Klug, L. E. Alexander, X–Ray Diffraction Procedures, 2–nd Edition, Wiley and Sons Inc., New–York, 1974.
[30] C. J. Brinker, G. V. Scherer, Sol-gel science, San Diego: Academic Press, 1990.
[31] C. Caizer, I. Hrianca, Eur. Phys. J. B, **31**, 391 (2003).
[32] J. M. D. Coey, D. Khalafalla, phys. status solidi (a) **11**, 229 (1972).